

# Use of multicompartmental models to measure rates of triglyceride metabolism in rats

NOME BAKER and MICHAEL C. SCHOTZ\*

Radioisotope Research, Veterans Administration Center and Department of Biological Chemistry, University of California Medical Center, Los Angeles, California

**SUMMARY** Specific activities and total radioactivity of liver and serum triglycerides were determined, in glucose-fed rats, at various times after a single intravenous injection of palmitate-1-C<sup>14</sup>. A multicompartmental model of plasma and liver triglyceride metabolism was constructed which was compatible with the known physiological and biochemical behavior of triglycerides and the observed data. The rates of triglyceride transfer from one compartment to another and the compartment sizes were calculated using a digital computer.

Analysis of the data showed that liver was composed of at least two triglyceride compartments, only one of which secreted triglycerides into plasma. Under these experimental conditions, virtually the entire liver turnover of triglycerides was accounted for as secretion into plasma. This rate of secretion was 0.27 mg/min per 100 g body weight. Only 22% of the newly formed liver triglycerides were synthesized directly from plasma free fatty acids.

**T**HE BIOCHEMICAL steps in the formation and utilization of triglyceride have been studied extensively *in vitro* (1). However, the mechanisms which regulate the rates of triglyceride (TG) metabolism and transfer are less well understood. Several laboratories have attempted to study the rates at which TG fatty acids are transferred from one compartment of the body to another *in vivo* using simple models of TG metabolism as a basis of calculation (2-4). Two important aspects of hepatic TG metabolism have not been incorporated into these earlier models: (a) There is a time delay in the secretion of newly synthesized hepatic TG into plasma (2, 3, 5, 6); (b) triglycerides that are located in

different subcellular structures do not always mix rapidly enough to be considered as a single homogeneous compartment (3, 7).

As a first step in our studies of dietary, hormonal, and drug influences on the metabolism of TG *in vivo* we have developed a model that is consistent with observed data and allows calculation of rates of hepatic synthesis, secretion, and utilization and of transfer of endogenous plasma TG to extrahepatic and hepatic tissues. In the present paper the model has been employed to determine these parameters in rats injected with palmitate-1-C<sup>14</sup>.

## METHODS

Twenty-one male Sprague Dawley rats weighing  $171 \pm 17$  g (mean  $\pm$  SD) were deprived of food but had free access to 10% glucose solution in place of drinking water for 20-24 hr prior to injection of C<sup>14</sup>. Fifteen minutes before C<sup>14</sup> fatty acid injection they were force-fed 2 ml of a 50% glucose solution.

Palmitic acid-1-C<sup>14</sup> (8.87 mc/mole; Volk Radiochemical Co., Chicago 40, Ill., Lot No. 11970) was complexed to bovine albumin (Fraction V, Armour Pharmaceutical Co., Kankakee, Ill.) according to the procedure of Friedberg et al (8). The final solution of the albumin complex contained 9.2  $\mu$ c/ml.

All rats were lightly anesthetized with ethyl ether, injected with 4.6  $\mu$ c of the albumin complex via the tail vein, and then permitted to recover from the anesthesia. The rats were again anesthetized lightly with ether, and blood was collected from the abdominal aorta at varying times. The liver was quickly removed and weighed and a lipid extract was prepared from a 1 g aliquot (9). Lipid extracts of 1 ml of serum were prepared as described by Sperry (10). Exactly 2 ml

\* With the mathematical and technical assistance of A. Satin, M. Chavez, and C. Weinstein. The mathematical treatment present in the Appendix was performed by Dr. R. Catura.

This work was reported in part at the Federation of American Societies for Experimental Biology (29).

of chloroform were added to the dried, washed liver lipid extracts whereas 0.1–0.2 ml chloroform was added to the serum extracts. All samples were stored under nitrogen at 4°. Where possible plasma and liver data for each time point were obtained on a given day.

The liver and serum TG were isolated by thin-layer chromatography. Plates for thin-layer chromatography were prepared by adding 50 ml of distilled water to 15 g Silica Gel G (E. Merck, Darmstadt, Germany), swirling in a flask, filtering through a layer of gauze, and immediately spreading over five 20 x 20 cm glass plates using the Stahl applicator (C. Desaga, G.m.b.H., Heidelberg, Germany). The silicic acid plates were air-dried, activated at 125° for 2 hr, and stored in a dust-free atmosphere of low humidity.

All spots and streaks were applied to the plates quantitatively with a 100 µl Hamilton syringe, 35 cm from the bottom of the plate. Forty microliters of liver extract, described above, was evenly distributed at the origin in an area about 2.5 x 0.3 cm. In the case of rat serum, the entire lipid extract from 1 ml of serum in chloroform was streaked across the plate (16 x 0.3 cm).

Development of the silicic acid plates was carried out in glass tanks (21 x 21 x 9.5 cm). The developing solvent (2 ml glacial acetic, 32 ml ethyl ether, and 166 ml *n*-hexane) was equilibrated in the tank for a minimum of 1 hr. The plates were developed by ascending chromatography for 60–70 min. After development, the plates were air-dried and exposed to iodine vapor for 10–20 sec at room temperature. The TG spots were outlined with a pencil, carefully scraped with a razor blade onto smooth paper, and quantitatively transferred into a 15 ml ground-glass stoppered test tube. At least 5 min were allowed for the coloration due to iodine to fade before scraping the plates. Quantitative elution of the TG was accomplished by adding 10 ml of chloroform to the silicic acid scrapings, shaking vigorously for 1 min, and filtering through fat-extracted filter paper. Aliquots were assayed for TG (11) and for radioactivity in a Packard liquid scintillation counter. Recovery of labeled and unlabeled TG using this method was 95%.

Specific activity (per cent injected dose per milligram TG, normalized to 100 g body weight) was calculated as follows:

$$(\text{cpm/mg TG}) \times (\text{body weight}/100) \times (100/\text{cpm injected}).$$

Total activity of liver TG (per cent of injected dose; not corrected for body weight) was calculated by multiplying average specific activities at a given time by the mean liver TG content (milligrams TG per total liver/100 g body weight) for all the rats used in this study. Total serum TG activity (per cent of injected

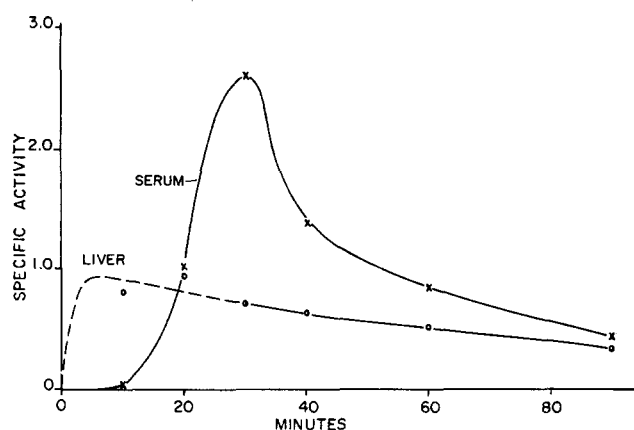


FIG. 1. Rat liver and serum TG specific activities following palmitate-1-C<sup>14</sup> injection. Three rats were used for each point in time and the mean specific activity was plotted. The broken-line portion of the liver TG curve during the first 20 min indicates that the initial rise is not well defined. Units of specific activity are defined in the text. See Fig. 4 for variance.

dose; not corrected for body weight) was determined by multiplying the average serum TG specific activity at each time by the serum volume per 100 g body weight, i.e., 4.0 ml (12), and then by the mean serum TG concentration (milligrams/milliliter) for all rats used in the study.

## RESULTS

Liver and serum TG specific activity–time curves during the first 90 min following intravenous injection of palmitate-1-C<sup>14</sup> are shown in Fig. 1. The liver TG specific activity rose rapidly and at 10 min reached a value which was not significantly different from the 20-min point. The rapid rise in liver TG specific activity has been observed in diverse physiological and dietary states (2, 3, 5, 13) and may be predicted from the known rapid turnover of its labeled precursor, plasma free fatty acid (FFA). Serum TG was virtually unlabeled for at least 10 min after palmitate-C<sup>14</sup> injection. Following this lag period, labeled TG entered the plasma at a rapid rate, as indicated by the steep rise in serum TG specific activity between 10 and 20 min. At 20 min the liver and serum TG specific activities were not significantly different from each other; however, the serum TG specific activity continued to rise to a value about twice the highest liver value. The serum TG specific activity reached a maximum 30 min after labeled fatty acid injection, and then decreased (up until 90 min after injection) at a rate considerably greater than that of the liver at any time. The decline of the serum specific activity curve was a complex exponential function of time; during the last hour of study the slopes of both liver and serum curves were significantly less than during

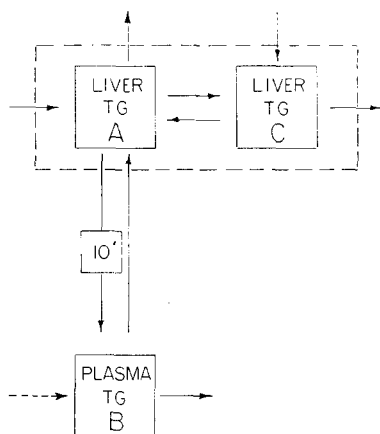


FIG. 2. A simple model of TG metabolism. Compartments *A* and *C* represent liver TG. Compartment *B* represents the plasma TG. A 10-min delay in hepatic TG secretion into plasma is indicated (arrow into *B* from *A*).

the preceding hour. The mean serum and liver TG values for the 21 rats were 0.96 ( $\pm 0.26$ ) and 22.1 ( $\pm 9.0$ ) mg/100 g body weight ( $\pm$ SD), respectively. The average serum TG concentration was 0.24 mg/ml, and the average liver weight for the 171 g rats employed was 7.5 g.

## THEORETICAL CONSIDERATIONS

### *Description of a Minimal Model*

One of the simple models compatible with the observed data and the known physiological behavior of TG is shown in Fig. 2. Three TG compartments are shown: *A* and *C*, both located in the liver, and *B*, plasma TG. Laurell had earlier constructed a model of TG metabolism in which hepatic TG was considered as a single homogeneous pool (2). However, the present data (Fig. 1) as well as those of other workers (5, 7, 13, 14) are clearly incompatible with the concept that a simple precursor-product relationship (15) exists between total liver TG and plasma TG in the rat. Rather, the data indicate that the liver is a heterogeneous compartment, only part of which may serve as a plasma TG precursor (Fig. 2). (The plasma TG compartment has also been shown recently to be heterogeneous in fed and fasted rabbits (3). Additional experiments will be required to assess the error that results from our having treated the plasma TG compartment as though it were homogeneous.)

Liver TG is derived in part from plasma TG (2, 16). Another inflow into pool *A* represents liver TG derived from plasma FFA (17) and from a variety of other lipid and nonlipid sources. Hepatic TG is also shown as entering pool *C*. Compartment *C* differs from *A* in that newly formed TG which is synthesized from

palmitate- $C^{14}$  in the liver does not enter *C* directly. Hepatic TG is shown as leaving compartments *A* and *C* by undesignated mechanisms, e.g. by hydrolysis and subsequent oxidation, by esterification, or by transesterification (16). In the present study we are primarily concerned with a third exit from the liver TG compartment, namely hepatic TG secretion into plasma (Fig. 2; arrow into *B* from *A*). A ten minute delay in the exit of TG from liver is indicated, to take into account the results shown in Fig. 1. Finally, an arrow leaving the plasma TG compartment is shown, to allow for plasma TG conversion to compounds other than liver TG, including possibly some other hepatic lipids.

An additional inflow into plasma TG (dotted arrow) from extrahepatic sources is also noted in the model. We have assumed that in the absence of dietary fat this rate is small compared to the rate of hepatic TG secretion (5, 6, 18) and have ignored it in final evaluation of the TG flux into and out of plasma.

### *Solution of the Minimal Model*

The model shown in Fig. 2 was used as the basis for formulating a mathematical expression that would allow the calculation of the rate of TG secretion into plasma. The differential equations and a limited solution of these equations are given in the Appendix. Data at four different times are needed for a solution. Seven data points which we obtained allowed us to calculate an average value based upon different combinations of four data points. Using the first three data points in each solution and varying the fourth, we obtained four values for the rate of hepatic TG secretion into plasma, the average of which was found to be 0.46 mg/min per 100 g body weight.

### *Construction of a More Complex Model*

A multicompartmental model which has proved useful in calculating rates of TG flux in the intact rat is shown in Fig. 3. It was designed to permit solution by the digital computer program of Berman et al. (19). It differs from the model in Fig. 2 only in that the 10 min minimum delay (Fig. 2) is specifically accounted for by assuming that newly synthesized liver TG (and TG which enters this compartment from plasma TG and from other sources) must pass through a series of small TG compartments (5-12 in Fig. 3) within the liver before it is secreted into plasma. We consider that passage through the endoplasmic reticulum of liver cells could be a possible physiological basis of this assumption. The maximum number of compartments is restricted by the computer program; therefore, only 8 TG delay pools could be employed. Compartments 3, 4, and 13 in Fig. 3 correspond to *A*, *C*, and *B*, respectively in Fig. 2.  $C^{14}$  input into hepatic TG in the expanded

model is specifically indicated by the introduction of a plasma FFA compartment, 1, interchanging with an additional compartment, 2, representing extrahepatic tissue lipids. The latter represents recycling of label into the FFA compartment, which is known to occur (2, 3). In the fed rat, a part of the label introduced into the FFA pool is thought to be derived from intravascular hydrolysis of TG. This is not shown in the model; however, the relationship indicated between compartments 1 and 2 represents mathematically the equivalent process. No attempt to evaluate the rate of recycling was made in this study. Influxes into hepatic TG from sources other than plasma FFA and TG are designated by arrows into compartments 3 and 4. These carbon inflows have been assumed to be relatively unlabeled.

### Initial Estimates of Parameters

The program of Berman et al. (19) requires that initial estimates of all rate constants be presented to the computer. The computer can then calculate radioactivity in each compartment at varying times and compare the calculated values with the experimental data. It then changes the initial estimates repeatedly and gradually until a set of rate constants is obtained that is consistent with the observed data. The final set of rate constants that the computer analysis yields is not dependent upon assumptions that are made in order to arrive at initial estimates, provided the rate constants are allowed to vary. However, careful estimation of rate constants allows a solution to be reached much more quickly than if random initial estimates are used. By way of example, we have indicated in the following paragraph the basis of our initial estimates, all of which were allowed to vary at some time. In a complex model such as that used here, it was expeditious to carry out a preliminary run (two iterations) and then to vary only

those rate constants that would theoretically affect the shape of the poorly fitting portion of the curve. Subsequent computations were then run in which two to five parameters were varied at a time to evaluate the accuracy of the estimated rate constants.

The initial estimate for total turnover rate constant of the plasma TG pool was based upon unpublished experiments in which Triton was administered to glucose-fed rats and the plasma TG accumulation noted for 90 min. Assuming a plasma volume of 4.0% body weight (12) and assuming that Triton produced a 100% block in the removal of TG from plasma, the amount of TG which accumulated in the plasma in 90 min required that it be secreted into the liver at a minimal rate of 0.15 mg/min per 100 g body weight (fractional rate constant = 0.16/min). Laurell found that C<sup>14</sup>-labeled endogenous TG of glucose-fed rats (258–306g) was replaced at a fractional rate constant of 0.08–0.20/min (2). Belfrage, Borgström, and Olivecrona (20) obtained steeper disappearance curves than Laurell, using TG-C<sup>14</sup>-labeled chyle (4–33 mg TG load) in glucose-fed rats weighing 210 g. Their values ranged from 0.20–0.33/min. Assuming that the plasma TG fractional turnover rate might be inversely related to body weight, and taking into account differences in feeding of glucose and in the form of administering C<sup>14</sup>-labeled TG, we estimated that the plasma TG fractional turnover rate of 171-g rats should fall within the range of 0.16–0.40/min. One-third of the TG that leaves plasma at any time was initially estimated (on the basis of calculations made using data from French and Morris (21)) to enter the liver TG pool. Data presented by Stein and Shapiro (16) are consistent with this estimate. Since the specific activity–time curve of pool 3 was not directly determined, a rough estimate of its turnover rate constant had to be obtained from the falling slope of plasma TG. This estimate is based on the consideration that

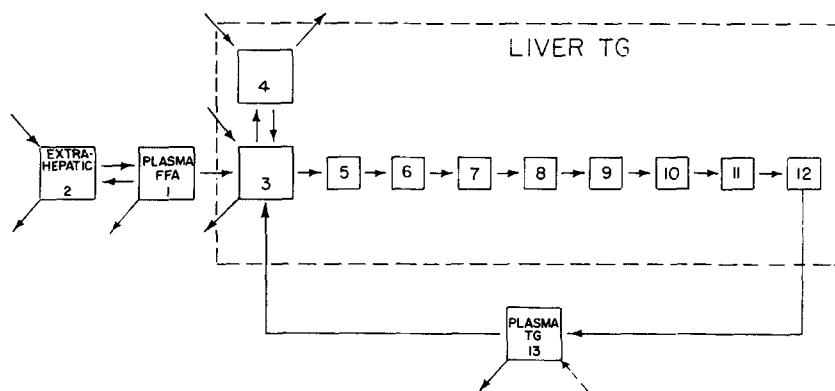


FIG. 3. A multicompartmental model of TG metabolism. Liver TG is represented by the compartments enclosed within broken lines.

the early fall in plasma TG specific activity should reflect the slope of its immediate precursor, delay compartment 12, which indirectly reflects the slope of each of the preceding precursor compartments, including compartment 3. The slope of the plasma TG specific activity-time curve shortly after reaching its maximum was approximately 0.1/min. The rate constants of the 8 delay pools were set equal to each other and assumed to be large enough to bring about the observed 10 min delay (values ranging from 0.4–1.0/min per compartment were tried). The sum of exit rates from liver TG compartments 3, 4, and 12 divided by the total amount of liver TG should approximate the slope of the whole liver specific activity-time curve at the latest time studied (about 0.007/min,  $t = 90$ –150 min). By assuming that: (a) approximately half the liver's TG was confined to the slowly turning-over (3, 7) compartment 4, (b) the unlabeled influx into 13 from outside the system was zero (5, 6, 18), and (c) that the rates (milligrams per minute) of TG oxidation, hydrolysis, etc., from compartments 3 and 4 were equal, we were able to calculate, from steady-state equations, the

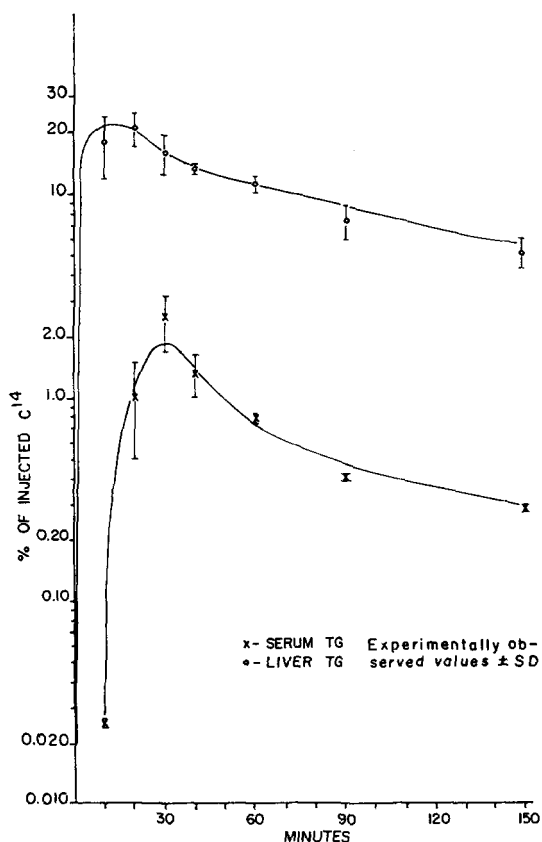


FIG. 4. Calculated vs. observed TG- $C^{14}$  in serum and in liver as a function of time after injection of palmitate-1- $C^{14}$ . The curves (solid lines) were computed by the program of Berman et al. (19) using the parameters shown in Fig. 5.

initial estimates of the rate constants for each of the arrows shown in Fig. 3 except those relating to the FFA compartment 7. The latter values were based upon a solution of the data presented by Olivecrona et al (22). The fraction of the plasma FFA turnover rate directed into compartment 3 was adjusted so that approximately 20% of the injected  $C^{14}$  would be converted to hepatic TG in the first few minutes after the injection. The initial estimates for the rate constants into compartment 2 from 7 and out of compartment 7 into undesignated compartments were made by difference and by assuming that the latter two rate constants were equal. The fractional turnover rate of compartment 2 was assumed (based on inspection of Laurell's data (2)) to be an order of magnitude smaller than that of 7. The FFA pool size in the glucose-fed rat was obtained from Laurell's data (2).

We would like to reemphasize that initial estimates of rate constants are used as a starting point from which the computer may then make better estimates by iterative procedures. Thus, although we assumed as an initial estimate that the rates of TG metabolism in compartments 3 and 4 were equal the computer analysis subsequently showed (see below) that these rates probably are unequal. On the other hand the reader should note that two rate constants were not allowed to vary at any time during the analysis. These were the rate constants of (a) FFA leaving plasma and entering compartment 2, and (b) FFA entering undesignated compartments. Therefore, these rate constants are not determined by the present analysis. Numerical values are presented only as a basis for further study. Variation of these rates has little influence on calculated rates of hepatic TG secretion and of plasma TG turnover.

#### Evaluation of the TG Flux Rates

After numerous computer trials with different initial estimates for the various rate constants we obtained a set of values for the model of Fig. 3 which defined the serum and liver TG- $C^{14}$ -time curves shown in Fig. 4. The correspondence between the experimentally observed values and the calculated curves is generally good, with the exception of the 30 min serum value. We were unable to find a set of values that would allow the serum curve to reach the observed value without causing serious displacement of other portions calculated from the experimental curve. (Two of the three experimental serum TG- $C^{14}$  values at 30 min agreed with the calculated value; the one high value may have been spurious.)

The set of parameters used to obtain the calculated curves is presented in Fig. 5. Several of these values are noteworthy. First, the value of 0.26 mg TG/min per

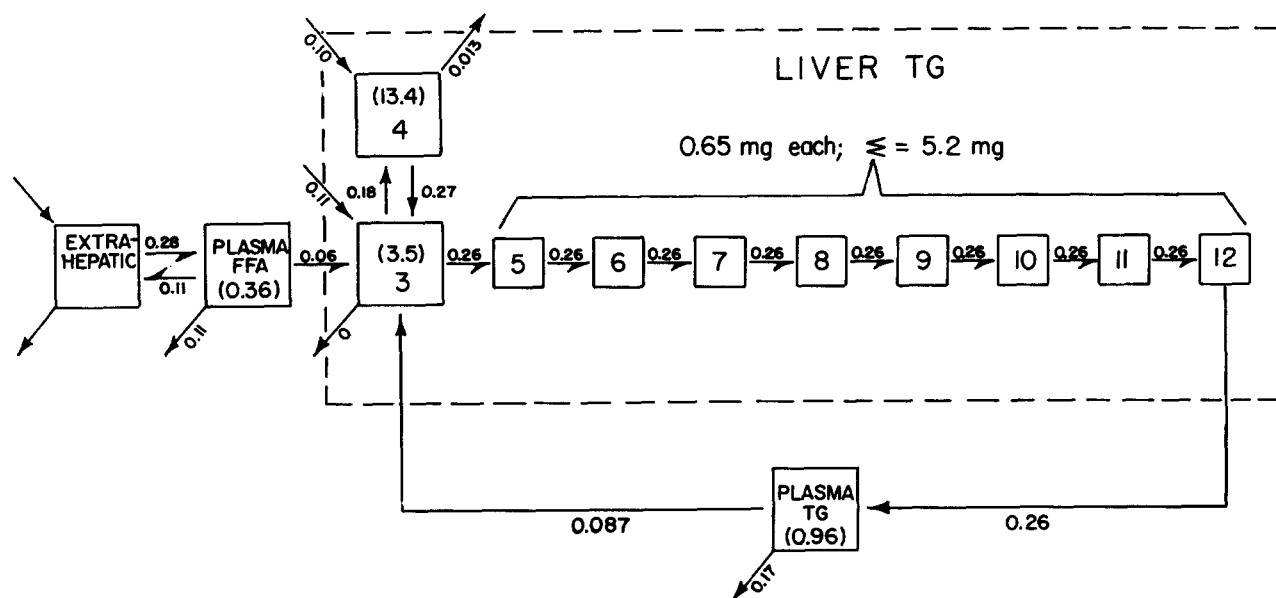


FIG. 5. Summary of compartment sizes and rates of transfer and metabolism. Compartment sizes are expressed as mg TG or FFA per 100 g body weight; except for "delay pools" 5-12, compartment sizes are in parentheses. Rates are expressed in mg TG or FFA per 100 g body weight per min. These values, when used with the program of Berman et al. (19), are the basis of the calculated curves shown in Fig. 4.

100 g body weight for the hepatic TG secretion rate is in the middle range of values that are predictable from the removal rate of TG- $C^{14}$ -labeled chyle in the glucose-fed rats of Belfrage et al. (20), if one assumed chyle TG were removed at the same rate constant as endogenous plasma TG. Second, the sum of all the liver TG efflux (including hydrolysis, etc.) from pools 3-12 inclusive = 0.013 (from 4) + 0 (from 3) + 0.26 (from 12) = 0.27 mg/min per 100 g body weight. Thus virtually the entire hepatic TG turnover is accounted for by TG secretion into serum. Third, replacement of the TG that leaves the liver each instant can be accounted for only to a relatively minor extent by plasma FFA conversion to hepatic TG (0.06 mg FFA/min per 100 g body weight, Fig. 5). In terms of hepatic TG formation, about  $0.06/0.27 \times 100 = 22\%$  of the newly formed hepatic TG is derived from plasma FFA; 32% is formed from plasma TG; and 46% is derived from other sources.

## DISCUSSION

Following the intravenous injection of palmitate- $1-C^{14}$  albumin into glucose-fed rats radioactivity is quickly incorporated into liver TG. However, as noted independently by other workers (2, 3, 5, 14), a 10 min delay occurs before the newly synthesized TG is secreted into plasma. Measurement of plasma and liver TG specific activities at different times indicated that the liver compartment which secreted TG had a specific activity

considerably higher than that of the liver as a whole. This observation, which has also been made in other laboratories (3, 5, 14), is consistent with the heterogeneity of the hepatic TG compartments first noted by Stein and Shapiro (7). On the other hand it was incompatible with the model proposed by Laurell (2), in which liver acted as a simple well mixed precursor pool that supplied plasma with its TG. Since model building is necessary if the data are to be used as a means of quantifying rates of TG secretion, we constructed an alternative model compatible with our observed data and with the known physiological and biochemical fate of fatty acids and TG. Because of a lack of experimental data concerning several aspects of TG metabolism, the construction of any single complex model was ambiguous. For example, we have assumed in building the model of Fig. 3 that both plasma FFA and plasma TG enter a common liver TG compartment (7, 17). It is not known whether this is true. Another possible model that might just as well have been employed is shown in Fig. 6A (plasma FFA and TG enter into different liver TG compartments which do not equilibrate immediately). Another possible model (Fig. 6B) which cannot be excluded is one in which newly synthesized hepatic TG passes through a series of small delay pools before entering a larger pool which could serve as the immediate plasma TG precursor. Specific construction of the various models, we feel, is valuable in that each model predicts specific activity-time curves and pool sizes for each liver TG

compartment. Further experiments should allow selection of a more correct model.

Fortunately, neither the choice of models nor the assumed proportion of TG turnover due to hepatic TG uptake appreciably influences the estimated values (using the program of Berman et al. (19)) for the rates of TG synthesis from plasma FFA, of total liver TG turnover, or of hepatic TG secretion into the circulation. The insensitivity of the final calculations of these particular parameters to the choice of model is perhaps more apparent from closer inspection of the liver and serum specific activity-time curves (Fig. 1). The peak liver TG specific activity (which should theoretically

plasma) TG turnover is approximated by the terminal slope of the total liver specific activity curve regardless of the model. Finally, the rate of hepatic secretion is approximated by (a) the falling slope of the plasma TG specific activity-time curve immediately after it reaches its maximum (this curve theoretically approximates the rate constant of turnover of that part of the liver TG which serves as a plasma TG precursor), (b) the time required for the plasma TG specific activity to reach its maximum once it starts its rapid rise (see eq. 4 in reference 23), and (c) the size of the plasma TG compartment. This is true for each model that has been considered so far.

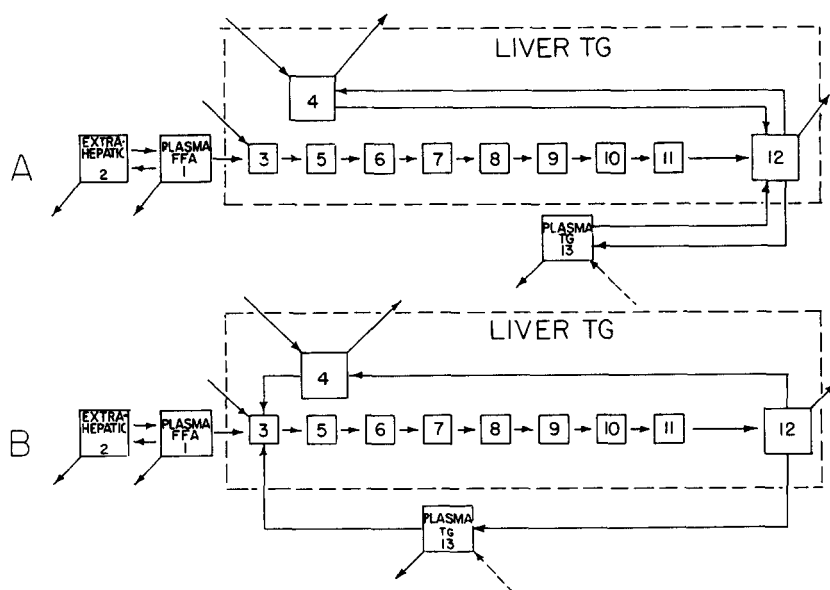


FIG. 6. Two alternative models of TG and FFA flux between liver and plasma compartments. In both models TG which is newly derived from plasma FFA passes through a series of delay pools (3-12) immediately upon entering the liver (see Fig. 3). In model A, plasma TG which enters the liver is considered to enter a different hepatic TG compartment than that which is derived from plasma FFA. Models A and B differ in the relationships between compartments 3, 4, 12, and 13.

be reached within 10 min) primarily determines the calculated rate of liver TG synthesis from plasma FFA regardless of the choice of model:

$$R \approx \frac{\alpha Q \lambda_{11}}{100 (1 - e^{-10\lambda_{11}})}$$

where:  $R$  = mg plasma FFA converted to liver TG per min per 100 g body weight

$\alpha$  = activity in liver at  $t = 10$  min

$Q$  = mg FFA in plasma

$\lambda_{11}$  = fractional turnover rate constant of plasma FFA compartment by all exits.

Similarly, the total rate constant of liver (or liver and

Although the choice of models does not appreciably influence the estimated values for several rates that we wished to measure, one of these rates, milligrams FFA converted to hepatic TG/min per 100 g body weight, is dependent upon values derived from the literature. The degree of error may be estimated by use of the preceding expression. If the value used for plasma FFA compartment size were 25% too great and if the rate constant of plasma FFA turnover were in error by 25% in the same direction, an overestimate of about 50% in this rate would be made. On the other hand, errors in opposite direction for the rate constant  $\lambda_{11}$ , and for the compartment size  $Q$ , would tend to cancel each other. The ratio  $\lambda_{21}/\lambda_{11}$  is calculated from our

own observed data by the computer analysis. Over-all rates of TG turnover, secretion, and formation are independent of the accuracy of either  $\lambda_{11}$  or  $Q$ , and, as shown in the Appendix, no information regarding the kinetics of the FFA compartment is needed to calculate the rate of hepatic TG secretion. Another value that relies upon data taken from the literature is the rate of hepatic TG formation directly from plasma TG. If one-fifth or one-half (instead of the assumed one-third) of plasma TG which turns over is incorporated into liver TG the rate would be modified from 0.087 to 0.052 or 0.13 mg TG/min per 100 g bodyweight, respectively, and the rate of plasma TG disappearance to extrahepatic tissues would be changed from 0.17 to 0.21 or 0.13, respectively. The calculated rates of hepatic TG secretion and of total plasma TG turnover would remain virtually unchanged.

A number of other workers have injected palmitate- $C^{14}$  into animals to study hepatic and plasma TG interrelations. Most of these studies indicated (as did the present one) that liver TG was contained in separate compartments which mixed poorly. This supports Stein and Shapiro's earlier observation (7). Some investigators have suggested that in rabbits (3) and in man (24) not only the various subcellular liver fractions but also the serum low density lipoprotein TG may all be treated as a single well mixed homogeneous pool of TG. However, data to support this assumption are not available in man, and in some rabbits the assumption of homogeneity is not applicable (5). The data of Lombardi and Schotz (25) indicate that in young rats fed once a day for 1 hr the liver TG pool may approximate a single well mixed compartment. Further experiments are required to establish conditions which might either permit the various hepatic pools to mix rapidly with each other or allow the slowest mixing pool to diminish in size so that its contribution to the total liver TG behavior becomes negligible.

Maling et al. have also presented evidence which should bear on this point; however, in their studies (see reference 14, Fig. 5) TG in the liver does not appear to acquire  $C^{14}$  at an appreciable rate during the first 20 min after the intravenous injection of palmitate- $C^{14}$ . This observation does not agree with observations made in other laboratories. In our experience (unpublished), the liver specific activity 10 min after an intravenous injection of palmitate- $C^{14}$  has a value which does not differ significantly from the 20 min value under a variety of experimental conditions.

The rates of hepatic TG secretion, formation, and utilization in the glucose-fed rat (Fig. 5) were compatible with previously published observations which indicate that in glucose-fed animals TG continues to be secreted into the circulation (2), hepatic lipogenesis

from carbohydrate increases (compared to fasted rats) (26), and oxidation of fatty acid is depressed (27). If the estimates, taken from the literature, of FFA compartment size and turnover time are accurate, our findings indicate that in the fed state only a small proportion of newly synthesized hepatic TG is derived directly from FFA.

Two different values, depending on the approach used, were obtained for the hepatic TG secretion rate. If the 10 min time delay were considered to result from a slow passage of newly synthesized TG through an intracellular channel in which no intermixing with hepatic TG occurred (model of Fig. 2), the calculated rate of hepatic TG secretion was higher than that obtained using the more complicated model of Fig. 3. Tentatively, we propose to use the latter model for comparison of triglyceride metabolism in various dietary, hormonal, and metabolic states, since it is more convenient to use, despite its greater complexity, and provides a more complete solution of the model. However, further study of the detailed physiology of hepatic triglyceride secretion will be necessary before its validity is established.

## APPENDIX

The derivation and treatment of equations which were used to determine the rate of hepatic TG secretion into plasma for the minimal model shown in Fig. 2 and based upon the data shown in Figs. 1 and 4 are given in the following presentation.

Compartment size (labeled plus unlabeled material) will be designated by  $Q_i$  and the radioactivity within it at any time,  $t$ , by  $q_i(t)$ . Let the flow rate,  $K_{ij}$ , be the quantity of material (labeled plus unlabeled) flowing into compartment  $i$  from compartment  $j$  and  $K_{ii}$  be the total flow rate of material out of compartment  $i$  via all pathways. The rate constants  $\lambda_{ij}$  and  $\lambda_{ii}$  are defined as follows:

$$\lambda_{ij} = \frac{K_{ij}}{Q_j} \quad \lambda_{ii} = \frac{K_{ii}}{Q_i}$$

The composite of compartments  $A$  and  $C$ , indicated by the broken line in Fig. 1, is defined as the total liver triglyceride compartment. Its size,  $Q_l$ , and specific activity,  $S_l(t)$ , are given by the following equations:

$$Q_l = Q_a + Q_c$$

$$S_l = \frac{q_a(t) + q_c(t)}{Q_l} \quad (1)$$

All compartment sizes and flow rates are considered to be constant in time. On the basis of experimental data, a 10 min time delay is assumed in the flow of material from compartment  $A$  to compartment  $B$ ; i.e., radioactivity leaving compartment  $A$  via the pathway designated  $\lambda_{ba}$  at time  $t$  enters compartment  $B$  at time  $t + 10$ . The flow represented by  $\lambda_{co}$  is assumed to



contain no radioactivity. At zero time, radioactivity is injected into an exterior compartment and enters the system at an unknown rate through the pathway designated  $\lambda_{ao}$ .<sup>1</sup> The boundary conditions are  $q_a(0) = q_c(0) = 0$  and, because of the time delay  $q_b(t) = 0$  for  $t \leq 10$ .

An analytic solution of the model is impossible because the rate at which radioactivity enters the system is unknown. Even if a functional form is assumed for this rate an analytic solution is complicated by the time delay. Therefore, a method of solution must be sought which does not depend explicitly upon the transport of radioactivity into compartment *A* from its exterior source and which is able to incorporate the previously mentioned time delay. The information available upon which to base a solution is knowledge of  $Q_b$  and  $Q_i$  and values of  $q_b(t)$ ,  $Q_b$ , and  $S_i(t)$ .

The differential equations describing the rate of change of radioactivity in compartments *B* and *C* are:

$$\frac{dq_b(t+10)}{dt} = \lambda_{ba}q_a(t) - \lambda_{bb}q_b(t+10) \quad (2)$$

$$\frac{dq_c(t)}{dt} = \lambda_{ca}q_a(t) - \lambda_{cc}q_c(t) \quad (3)$$

The corresponding equation for compartment *A* is not useful since the solution is to be independent of radioactivity transport into this compartment. If eq. (2) is solved for  $q_a(t)$  and this expression substituted into eq. (1) and (3), the following two equations result after minor simplifications:

$$Q_i S_i(t) = \frac{1}{\lambda_{ba}} \left[ \frac{dq_b(t+10)}{dt} + \lambda_{bb}q_b(t+10) \right] + q_c(t) \quad (1')$$

$$\frac{dq_c(t)}{dt} + \lambda_{cc}q_c(t) = \frac{\lambda_{ca}}{\lambda_{ba}} \left[ \frac{dq_b(t+10)}{dt} + \lambda_{bb}q_b(t+10) \right] \quad (3')$$

Equation (3') may be simplified by using the following equality:

$$\frac{dq}{dt} + \lambda_q = e^{-\lambda t} \frac{d(qe^{\lambda t})}{dt}$$

If eq. (3') is then multiplied by  $e^{\lambda_{cc}t}$  the left side may be readily integrated; the right side of the equation must be integrated by parts. After performing these integrations and applying boundary conditions on  $q_b$  and  $q_c$  the following equation results after simplification:

$$q_c(t) = \frac{\lambda_{ca}}{\lambda_{ba}} \left[ q_b(t+10) - (\lambda_{cc} - \lambda_{bb})e^{-\lambda_{cc}t} \int_0^t q_b(t+10)e^{\lambda_{cc}t} dt \right]$$

<sup>1</sup> Twenty-one flow rates and twelve compartment sizes are indicated in the final evaluation of the model. Most of these values are dependent upon choice of model; moreover, even using a single model it is difficult, considering limitations of data and complexity of the model, to assess how accurate each value is. Further experimental data may be expected to result in modification of these estimates. The several parameters discussed in the paper are those that we think are relatively insensitive to choice of model.

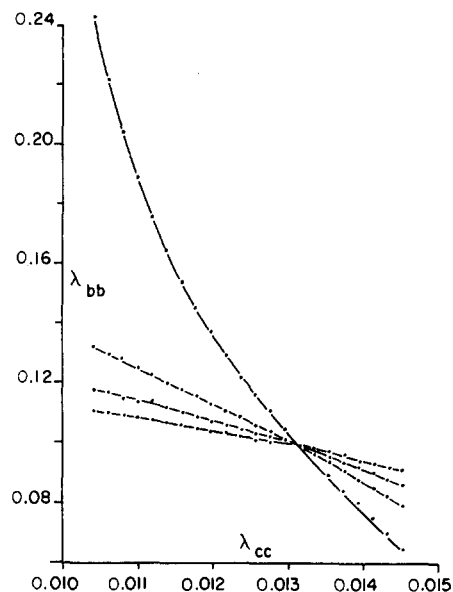


FIG. 7. A graph of the values of  $\lambda_{bb}$  (positive root values) obtained from solution of four quadratic equations as a function of the parameter  $\lambda_{cc}$ . The point of intersection indicates the value of  $\lambda_{cc}$  which makes the four equations obtained from eq. (3'') consistent.

Substituting this expression into eq. (1') and collecting terms one obtains:

$$Q_i S_i(t) = \frac{1}{\lambda_{ba}} \left[ \frac{dq_b}{dt}(t+10) + (\lambda_{bb} + \lambda_{ca})q_b(t+10) - \lambda_{ca}(\lambda_{cc} - \lambda_{bb})e^{-\lambda_{cc}t} \int_0^t q_b(t+10)e^{\lambda_{cc}t} dt \right] \quad (3'')$$

As mentioned previously, values of  $q_b(t)$  are known at a number of different times. By fitting these values with a sum of exponentials it is possible to obtain an analytic expression for  $q_b(t+10)$ . Using this expression time-dependent quantities on the right side of eq. (3'') may be evaluated. Since the left side of eq. (3'') is also known at a number of points in time, the only unknowns in this expression are the four rate constants ( $\lambda_{ba}$ ,  $\lambda_{ca}$ ,  $\lambda_{bb}$ , and  $\lambda_{cc}$ ). These lambdas are constant and must therefore satisfy this equation at any time for which it is evaluated. One may then evaluate the equation at four different times (a method discussed by Hart (28)) and obtain a solution for the lambdas from the four resulting equations. Since  $\lambda_{cc}$  appears in an exponent these equations are transcendental and a simple algebraic solution is impossible. For a given value of  $\lambda_{cc}$  there results an overdetermined set of four equations in three unknowns. For an arbitrary value of  $\lambda_{cc}$  these equations will not be consistent; i.e., values of  $\lambda_{ba}$ ,  $\lambda_{ca}$ , and  $\lambda_{bb}$  cannot be found which simultaneously satisfy all four equations. The solution consists of finding a value of  $\lambda_{cc}$  that makes the four equations consistent. This has been done in the present application by trial and error with the aid of a 7090 digital computer.

The rate constants  $\lambda_{ba}$  and  $\lambda_{ca}$  may be eliminated by combining any three of the four equations. The result is a quadratic equation in  $\lambda_{bb}$  with  $\lambda_{cc}$  appearing in the coefficients. Two such

combinations, together involving all four of the equations, are necessary to the solution. For a given  $\lambda_{cc}$  each of the two resulting quadratic equations yields values for  $\lambda_{bb}$ . The rate constant  $\lambda_{cc}$  is now treated as a parameter. The solution consists of varying  $\lambda_{cc}$  until the values of  $\lambda_{bb}$  obtained from the two equations agree. A graphical example of this agreement is shown in Fig. 7, using the data shown in Fig. 4. There are four unique combinations of the four equations taken three at a time. As mentioned above only two are necessary to solve the problem. In Fig. 7 the values of  $\lambda_{bb}$  obtained from solving all four of these combinations are plotted against  $\lambda_{cc}$ . The value of  $\lambda_{cc}$  for which these values agree is clearly 0.0132. Since the equations involving  $\lambda_{bb}$  are quadratic there are two solutions for each of them. Only the solutions involving the positive square root of the discriminant are shown in Fig. 2. The four solutions involving the negative root converge for the same value of  $\lambda_{cc}$ .

Using the values of  $\lambda_{cc}$  and  $\lambda_{bb}$  at the intersection point of the curves in Fig. 7 it is possible to solve for  $\lambda_{ba}$  and  $\lambda_{ca}$  from the equations combined to produce any particular quadratic equation. From the equations derived earlier and from others describing the fact that compartment sizes are unchanging in time one may solve for  $K_{ba}$ ,  $K_{ac}$ ,  $K_{bb}$ ,  $K_{cc}$ ,  $Q_a$ , and  $Q_c$ . Two different solutions result from the use of positive- and negative-root values of  $\lambda_{bb}$ . It is also possible to calculate  $q_a(t)$  and  $q_c(t)$  at a number of points in time.

An advantage of this method is that it does not depend on details of the differential equation describing a particular compartment. For this reason it is best applied in instances for which little is known about the transport of radioactivity between a compartment of the model and the exterior. It must be pointed out, however, that this method achieves only a partial solution. Since the solution contains only limited details of a particular compartment it can only produce limited information about it. Another feature of the analysis is that it incorporates a time delay involved in a flow rate. Although a delay of 10 min was used in the present application the solution allows it to be varied.

This method of solution involves experimental data from four points in time. The points were chosen as far as possible to represent the entire data. It is, of course, desirable to involve an arbitrary number of data points in the analysis and obtain a solution which best fits all of them.

The authors are grateful to Dr. Mones Berman and Dr. Thomas Olivecrona for advice and guidance in the initial stages of computer analysis. Also, we wish to thank Dr. Perri Stimson, VA Research Support Center, Sepulveda, Calif., for her mathematical assistance.

This study was supported in part by Public Health Service Research Grant A-4706 from the National Institutes of Health, United States Public Health Service.

Manuscript received September 5, 1963; accepted December 24, 1963.

#### REFERENCES

1. Wakil, S. J. *Ann. Rev. Biochem.* **31**: 369, 1962.
2. Laurell, S. *Acta Physiol. Scand.* **47**: 218, 1959.
3. Havel, R. J., J. M. Felts, and C. M. Van Duyne. *J. Lipid Res.* **3**: 297, 1962.
4. Friedberg, S. J., R. F. Klein, D. L. Trout, M. D. Bogdonoff, and E. H. Estes. *J. Clin. Invest.* **40**: 1846, 1961.
5. Borgström, B., and T. Olivecrona. *J. Lipid Res.* **2**: 263, 1961.
6. Havel, R. J., and A. Goldfien. *J. Lipid Res.* **2**: 389, 1961.
7. Stein, Y., and B. Shapiro. *Am. J. Physiol.* **196**: 1238, 1959.
8. Friedberg, S. J., W. R. Harlan, D. L. Trout, and E. H. Estes. *J. Clin. Invest.* **39**: 215, 1960.
9. Folch, J., M. Lees, and G. H. Sloane Stanley. *J. Biol. Chem.* **226**: 497, 1957.
10. Sperry, W. M. *Methods Biochem. Anal.* **2**: 106, 1955.
11. Van Handel, E. *Clin. Chem.* **7**: 249, 1961.
12. Metcalf, J., and C. B. Favour. *Am. J. Physiol.* **141**: 695, 1944.
13. Olivecrona, T. *Acta Physiol. Scand.* **54**: 295, 1962.
14. Maling, H. M., A. Frank, and M. G. Horning. *Biochim. Biophys. Acta* **64**: 540, 1962.
15. Zilversmit, D. B., C. Entenman, and M. C. Fishler. *J. Gen. Physiol.* **26**: 325, 1943.
16. Stein, Y., and B. Shapiro. *J. Lipid Res.* **1**: 326, 1960.
17. Laurell, S. *Acta Physiol. Scand.* **46**: 97, 1959.
18. Byers, S. O., and M. Friedman. *Am. J. Physiol.* **198**: 629, 1960.
19. Berman, M., M. F. Weiss, and E. Shahn. *Biophys. J.* **2**: 289, 1962.
20. Belfrage, P., B. Borgström, and T. Olivecrona. *Acta Physiol. Scand.* **58**: 111, 1963.
21. French, J. E., and B. Morris. *J. Physiol. (London)* **140**: 262, 1958.
22. Olivecrona, T., E. P. George, and B. Borgström. *Federation Proc.* **20**: 928, 1961.
23. Baker, N., W. W. Shreeve, R. A., Shipley, G. E. Incefy, and M. Miller. *J. Biol. Chem.* **211**: 575, 1954.
24. Havel, R. J. *Metabolism.* **10**: 1031, 1961.
25. Lombardi, B., and M. C. Schotz. *Proc. Soc. Exptl. Biol. Med.* **112**: 400, 1963.
26. Masoro, E. J., I. L. Chaikoff, S. S. Chernick, and J. M. Felts. *J. Biol. Chem.* **185**: 845, 1950.
27. Lossow, W. J., G. W. Brown, Jr., and I. L. Chaikoff. *J. Biol. Chem.* **222**: 531, 1956.
28. Hart, H. E. *Bull. Math. Biophys.* **17**: 87, 1955.
29. Schotz, M. C. *Federation Proc.* **21**: 292, 1962.